

Evidence for Neutral B Meson Decays to ωK^{*0}

P. Goldenzweig,² A. J. Schwartz,² I. Adachi,⁸ H. Aihara,⁴³ K. Arinstein,¹ V. Aulchenko,¹
 T. Aushev,^{18,13} S. Bahinipati,² A. M. Bakich,³⁹ A. Bay,¹⁸ I. Bedny,¹ V. Bhardwaj,³³
 U. Bitenc,¹⁴ A. Bondar,¹ A. Bozek,²⁷ M. Bračko,^{20,14} T. E. Browder,⁷ P. Chang,²⁶
 Y. Chao,²⁶ A. Chen,²⁴ K.-F. Chen,²⁶ B. G. Cheon,⁶ C.-C. Chiang,²⁶ R. Chistov,¹³
 I.-S. Cho,⁴⁸ Y. Choi,³⁸ J. Dalseno,⁸ M. Dash,⁴⁷ A. Drutskoy,² S. Eidelman,¹
 B. Golob,^{19,14} H. Ha,¹⁶ K. Hayasaka,²² H. Hayashii,²³ M. Hazumi,⁸ D. Heffernan,³²
 Y. Hoshi,⁴¹ W.-S. Hou,²⁶ Y. B. Hsiung,²⁶ H. J. Hyun,¹⁷ T. Iijima,²² K. Inami,²²
 A. Ishikawa,³⁵ H. Ishino,^{44,*} M. Iwasaki,⁴³ D. H. Kah,¹⁷ J. H. Kang,⁴⁸ T. Kawasaki,²⁹
 H. Kichimi,⁸ H. J. Kim,¹⁷ S. K. Kim,³⁷ Y. I. Kim,¹⁷ Y. J. Kim,⁵ K. Kinoshita,²
 S. Korpar,^{20,14} P. Križan,^{19,14} P. Krokovny,⁸ R. Kumar,³³ A. Kuzmin,¹ Y.-J. Kwon,⁴⁸
 S.-H. Kyeong,⁴⁸ J. S. Lange,⁴ J. S. Lee,³⁸ M. J. Lee,³⁷ S. E. Lee,³⁷ T. Lesiak,^{27,3} J. Li,⁷
 A. Limosani,²¹ S.-W. Lin,²⁶ C. Liu,³⁶ Y. Liu,⁵ J. MacNaughton,⁸ F. Mandl,¹¹
 S. McOnie,³⁹ K. Miyabayashi,²³ H. Miyata,²⁹ Y. Miyazaki,²² R. Mizuk,¹³
 T. Nagamine,⁴² E. Nakano,³¹ M. Nakao,⁸ H. Nakazawa,²⁴ S. Nishida,⁸ O. Nitoh,⁴⁶
 S. Ogawa,⁴⁰ T. Ohshima,²² S. Okuno,¹⁵ S. L. Olsen,^{7,10} W. Ostrowicz,²⁷ H. Ozaki,⁸
 P. Pakhlov,¹³ G. Pakhlova,¹³ H. Palka,²⁷ C. W. Park,³⁸ H. Park,¹⁷ H. K. Park,¹⁷
 L. S. Peak,³⁹ R. Pestotnik,¹⁴ L. E. Piilonen,⁴⁷ H. Sahoo,⁷ Y. Sakai,⁸ O. Schneider,¹⁸
 J. Schümann,⁸ C. Schwanda,¹¹ R. Seidl,^{9,34} A. Sekiya,²³ K. Senyo,²² M. E. Sevier,²¹
 M. Shapkin,¹² V. Shebalin,¹ C. P. Shen,⁷ J.-G. Shiu,²⁶ J. B. Singh,³³ A. Somov,²
 S. Stanič,³⁰ M. Starič,¹⁴ K. Sumisawa,⁸ T. Sumiyoshi,⁴⁵ S. Suzuki,³⁵ N. Tamura,²⁹
 M. Tanaka,⁸ Y. Teramoto,³¹ I. Tikhomirov,¹³ K. Trabelsi,⁸ S. Uehara,⁸ T. Uglov,¹³
 Y. Unno,⁶ S. Uno,⁸ P. Urquijo,²¹ Y. Usov,¹ G. Varner,⁷ K. E. Varvell,³⁹ K. Vervink,¹⁸
 C. C. Wang,²⁶ C. H. Wang,²⁵ M.-Z. Wang,²⁶ P. Wang,¹⁰ X. L. Wang,¹⁰ Y. Watanabe,¹⁵
 R. Wedd,²¹ J. Wicht,⁸ E. Won,¹⁶ B. D. Yabsley,³⁹ Y. Yamashita,²⁸ M. Yamauchi,⁸
 C. C. Zhang,¹⁰ Z. P. Zhang,³⁶ V. Zhulanov,¹ T. Zivko,¹⁴ A. Zupanc,¹⁴ and O. Zyukova¹

(The Belle Collaboration)

- ¹*Budker Institute of Nuclear Physics, Novosibirsk*
- ²*University of Cincinnati, Cincinnati, Ohio 45221*
- ³*T. Kościuszko Cracow University of Technology, Krakow*
- ⁴*Justus-Liebig-Universität Gießen, Gießen*
- ⁵*The Graduate University for Advanced Studies, Hayama*
- ⁶*Hanyang University, Seoul*
- ⁷*University of Hawaii, Honolulu, Hawaii 96822*
- ⁸*High Energy Accelerator Research Organization (KEK), Tsukuba*
- ⁹*University of Illinois at Urbana-Champaign, Urbana, Illinois 61801*
- ¹⁰*Institute of High Energy Physics,
Chinese Academy of Sciences, Beijing*
- ¹¹*Institute of High Energy Physics, Vienna*
- ¹²*Institute of High Energy Physics, Protvino*
- ¹³*Institute for Theoretical and Experimental Physics, Moscow*
- ¹⁴*J. Stefan Institute, Ljubljana*
- ¹⁵*Kanagawa University, Yokohama*
- ¹⁶*Korea University, Seoul*
- ¹⁷*Kyungpook National University, Taegu*
- ¹⁸*École Polytechnique Fédérale de Lausanne (EPFL), Lausanne*
- ¹⁹*Faculty of Mathematics and Physics, University of Ljubljana, Ljubljana*
- ²⁰*University of Maribor, Maribor*
- ²¹*University of Melbourne, School of Physics, Victoria 3010*
- ²²*Nagoya University, Nagoya*
- ²³*Nara Women's University, Nara*
- ²⁴*National Central University, Chung-li*
- ²⁵*National United University, Miao Li*
- ²⁶*Department of Physics, National Taiwan University, Taipei*
- ²⁷*H. Niewodniczanski Institute of Nuclear Physics, Krakow*
- ²⁸*Nippon Dental University, Niigata*
- ²⁹*Niigata University, Niigata*
- ³⁰*University of Nova Gorica, Nova Gorica*
- ³¹*Osaka City University, Osaka*

³²*Osaka University, Osaka*

³³*Panjab University, Chandigarh*

³⁴*RIKEN BNL Research Center, Upton, New York 11973*

³⁵*Saga University, Saga*

³⁶*University of Science and Technology of China, Hefei*

³⁷*Seoul National University, Seoul*

³⁸*Sungkyunkwan University, Suwon*

³⁹*University of Sydney, Sydney, New South Wales*

⁴⁰*Toho University, Funabashi*

⁴¹*Tohoku Gakuin University, Tagajo*

⁴²*Tohoku University, Sendai*

⁴³*Department of Physics, University of Tokyo, Tokyo*

⁴⁴*Tokyo Institute of Technology, Tokyo*

⁴⁵*Tokyo Metropolitan University, Tokyo*

⁴⁶*Tokyo University of Agriculture and Technology, Tokyo*

⁴⁷*Virginia Polytechnic Institute and State University, Blacksburg, Virginia 24061*

⁴⁸*Yonsei University, Seoul*

Abstract

We present the results of a study of the charmless vector-vector decay $B^0 \rightarrow \omega K^{*0}$ with 657×10^6 $B\bar{B}$ pairs collected with the Belle detector at the KEKB e^+e^- collider. We measure the branching fraction to be $\mathcal{B}(B^0 \rightarrow \omega K^{*0}) = [1.8 \pm 0.7(\text{stat})_{-0.2}^{+0.3}(\text{syst})] \times 10^{-6}$ with 3.0σ significance. We also perform a helicity analysis of the ω and K^{*0} vector mesons, and obtain the longitudinal polarization fraction $f_L(B^0 \rightarrow \omega K^{*0}) = 0.56 \pm 0.29(\text{stat})_{-0.08}^{+0.18}(\text{syst})$. Finally, we measure a large non-resonant branching fraction $\mathcal{B}(B^0 \rightarrow \omega K^+ \pi^-; M_{K\pi} \in (0.755, 1.250) \text{ GeV}/c^2) = [5.1 \pm 0.7(\text{stat}) \pm 0.7(\text{syst})] \times 10^{-6}$ with a significance of 9.5σ .

PACS numbers: 13.25.Hw, 12.15.Hh, 13.88.+e

The study of branching fractions and angular distributions of B meson decays to hadronic final states tests our understanding of both weak and strong interactions. Recently, B decays mediated by $b \rightarrow sq\bar{q}$ penguin amplitudes have received much attention in the literature. Unlike $b \rightarrow c$ spectator amplitudes (which are much better measured), penguin amplitudes contain an internal loop and thus are potentially sensitive to new propagators and couplings. Such mediating particles may have an energy scale too high to access directly. Several measured $b \rightarrow sq\bar{q}$ decays have yielded unexpected results; e.g., the decays $B \rightarrow \phi K^*$ and $B \rightarrow \rho K^{*0}$ are found to have large transverse polarization [1], and B decays to the closely related final states $K^+\pi^-$ and $K^+\pi^0$ exhibit different patterns of direct CP violation [2]. These results are difficult to accommodate within the Standard Model and may indicate the presence of new physics [3]. Furthermore, $b \rightarrow sq\bar{q}$ decays are useful for determining the angles ϕ_2 and ϕ_3 of the unitarity triangle [4].

In this Letter we present a study of the $b \rightarrow sd\bar{d}$ decay $B^0 \rightarrow \omega K^{*0}$. Theoretical calculations for the branching fraction cover the range $(0.3 - 10.0) \times 10^{-6}$ [5]. Experimentally, the 90% confidence level upper limit is 4.2×10^{-6} [6]. This analysis uses 605 fb^{-1} of data containing 657×10^6 $B\bar{B}$ pairs; this sample is almost three times larger than that used in Ref. [6]. The data was collected with the Belle detector [7] at the KEKB [8] e^+e^- asymmetric-energy (3.5 GeV on 8.0 GeV) collider with a center-of-mass (CM) energy at the $\Upsilon(4S)$ resonance. The production rates of $B^0\bar{B}^0$ and B^+B^- pairs are assumed to be equal.

The Belle detector is a large-solid-angle spectrometer. It includes a silicon vertex detector (SVD), a 50-layer central drift chamber (CDC), an array of aerogel threshold Cherenkov counters (ACC), time-of-flight scintillation counters (TOF), and an electromagnetic calorimeter (ECL) comprised of CsI(Tl) crystals located inside a superconducting solenoid coil that provides a 1.5 T magnetic field.

The B -daughter candidates are reconstructed through the decays $\omega \rightarrow \pi^+\pi^-\pi^0$, $K^{*0} \rightarrow K^+\pi^-$ and $\pi^0 \rightarrow \gamma\gamma$ [9]. A charged track is identified as a pion or kaon by using particle identification (PID) information from the CDC, ACC and TOF systems. We reduce the number of poor quality tracks by requiring that $|dz| < 4.0 \text{ cm}$ and $dr < 0.2 \text{ cm}$, where $|dz|$ and dr are the distances of closest approach of a track to the interaction point along the z -axis (opposite the direction of the positron beam) and in the transverse plane, respectively. In addition, we require that each charged track have a transverse momentum $p_T > 0.1 \text{ GeV}/c$ and a minimum number of SVD hits. Tracks matched with clusters in the ECL that are

consistent with an electron hypothesis are rejected.

Photons used for π^0 reconstruction are required to have energies in the laboratory frame greater than 50 (100) MeV for the ECL barrel (endcap), which subtends $32^\circ - 129^\circ$ ($17^\circ - 32^\circ$ and $129^\circ - 150^\circ$) with respect to the beam axis. We require π^0 candidates to have an invariant mass in the range $M_{\gamma\gamma} \in (117.8, 150.2)$ MeV/ c^2 and a momentum in the laboratory frame $p_{\pi^0} > 0.39$ GeV/ c .

We select ω mesons with an invariant mass in the range $M_{\pi\pi\pi} \in (0.730, 0.830)$ GeV/ c^2 , and K^{*0} mesons with $M_{K\pi} \in (0.755, 1.250)$ GeV/ c^2 . To reduce combinatorial background arising from low-momentum kaons and pions, we require that $\cos \theta_{K^{*0}} > -0.8$, where $\theta_{K^{*0}}$ is the K^{*0} helicity angle defined as the angle between the direction of the K^+ and the direction opposite to the B^0 momentum in the K^{*0} rest frame. The ω helicity angle, θ_ω , is defined as the angle between the normal to the three-pion decay plane and the negative of the B^0 momentum in the ω rest frame.

Signal decays are identified using the energy difference (ΔE) and the beam-energy-constrained mass (M_{bc}). These are defined as $\Delta E \equiv E_B - E_{\text{beam}}$ and $M_{bc} \equiv \sqrt{E_{\text{beam}}^2 - p_B^2}$, where E_{beam} denotes the beam energy and E_B and p_B denote the energy and momentum, respectively, of the candidate B -meson, all evaluated in the e^+e^- CM frame. We retain events satisfying $|\Delta E| < 0.2$ GeV and $M_{bc} \in (5.20, 5.29)$ GeV/ c^2 , and define a signal region $\Delta E \in (-0.10, 0.06)$ GeV, $M_{bc} \in (5.27, 5.29)$ GeV/ c^2 .

The dominant source of background is continuum $e^+e^- \rightarrow q\bar{q}$ ($q = u, d, s, c$) production. To discriminate relatively spherical $B\bar{B}$ events from jet-like $q\bar{q}$ events, we use 16 modified Fox-Wolfram moments (combined into a Fisher discriminant \mathcal{F} [10]), the CM polar angle between the B direction and the z -axis (θ_B), and the displacement along the z -axis between the signal B vertex and that of the other B in the event (ΔZ). Further discrimination is provided by a b -flavor tagging algorithm [11], which identifies the flavor of the B meson accompanying the signal candidate via its decay products: charged leptons, kaons, and Λ 's. This algorithm yields a quality factor r , which ranges from zero for no flavor discrimination to one for unambiguous flavor assignment.

We use Monte Carlo (MC) simulated signal [12] and data sideband events (defined as $M_{bc} \in (5.20, 5.26)$ GeV/ c^2 , $|\Delta E| < 0.2$ GeV) to obtain probability density functions (PDFs) for \mathcal{F} , $\cos \theta_B$ and ΔZ . These are multiplied together to form signal (\mathcal{L}_S) and $q\bar{q}$ background ($\mathcal{L}_{q\bar{q}}$) likelihood functions, and we require that $\mathcal{R}_{q\bar{q}} = \mathcal{L}_S / (\mathcal{L}_S + \mathcal{L}_{q\bar{q}})$ be above a threshold.

We divide the events into six bins of r and determine the optimum $\mathcal{R}_{q\bar{q}}$ threshold for each bin by maximizing a figure-of-merit $S/\sqrt{S+B}$, where S (B) is the number of signal (background) events in the signal region. This optimization rejects 99% of the $q\bar{q}$ background while preserving 50% of the signal.

The fraction of events having multiple candidates is 12%. We choose the candidate in an event to be the one that minimizes the quantity $|M_{\gamma\gamma} - m_{\pi^0}|$. This choice selects the correct candidate 90% of the time. We find that 9.6% of signal decays have at least one particle incorrectly identified but pass all selection criteria; these are referred to as “self-cross-feed” (SCF) events.

We obtain the yields using a four-dimensional (4D) extended unbinned maximum-likelihood (ML) fit to ΔE , M_{bc} , $M_{\pi\pi\pi}$ and $M_{K\pi}$. The likelihood function is given by

$$\mathcal{L} = \frac{e^{-(\sum Y_j)}}{N!} \prod_{i=1}^N \sum_j Y_j \mathcal{P}_j^i, \quad (1)$$

where Y_j is the yield of component j , \mathcal{P}_j^i is the PDF for component j , and i runs over all events in the sample. We include PDFs for the signal, $q\bar{q}$ background ($q\bar{q}$), charm B -decay background ($b \rightarrow c$), charmless B -decay background ($b \rightarrow s, u, d$), and non-resonant $B^0 \rightarrow \omega K^+ \pi^-$ decays. The MC acceptances for non-resonant $B^0 \rightarrow K^{*0} \pi^+ \pi^- \pi^0$ and $B^0 \rightarrow K^+ \pi^- \pi^+ \pi^- \pi^0$ are negligibly small and thus we do not consider these channels.

The PDF for each component is defined as $\mathcal{P}_j^i = \mathcal{P}_j(\Delta E^i) \mathcal{P}_j(M_{bc}^i) \mathcal{P}_j(M_{\pi\pi\pi}^i) \mathcal{P}_j(M_{K\pi}^i)$. For the signal and $\omega K^+ \pi^-$ components, we split the PDFs into two parts: $\mathcal{P}_j^i = (1 - f_{\text{SCF}}) \mathcal{P}_{\text{true}}^i + f_{\text{SCF}} \mathcal{P}_{\text{SCF}}^i$, where f_{SCF} is the SCF fraction (17% for $\omega K^+ \pi^-$), and “true” represents the correctly reconstructed decays. For the $q\bar{q}$, $b \rightarrow c$ and $b \rightarrow s, u, d$ backgrounds, no sizable correlations are found among the fitted variables. For the signal and $\omega K^+ \pi^-$ components, there are small correlations that are accounted for as described below.

The K^{*0} and ω resonances are modeled with Breit-Wigner functions whose widths are fixed to their PDG [13] values. The Breit-Wigner function used to describe the ω resonance is convolved with a Gaussian of $\sigma = 5.7$ MeV to take into account the detector resolution. This value, along with the means for both resonances and the fraction of $q\bar{q}$ background events containing ω ’s and K^{*0} ’s, are obtained from fitting the $M_{K\pi}$ and $M_{\pi\pi\pi}$ spectra of events in the data sideband.

All other PDF shapes are obtained from MC simulation. For the signal and $\omega K^+ \pi^-$ PDFs, the sum of a Crystal Ball line shape [14] and Gaussian is used to describe ΔE , and the

TABLE I: Signal yield Y and its statistical uncertainty, MC efficiency ε_{MC} , PID efficiency ε_{PID} , significance S with systematic uncertainties included, and measured branching fraction \mathcal{B} . For $\omega K^+\pi^-$, ε_{MC} and \mathcal{B} are for $M_{K\pi} \in (0.755, 1.250)$ GeV/ c^2 . For \mathcal{B} , the first (second) error is statistical (systematic).

Mode	Y	ε_{MC} (%)	ε_{PID}	S	\mathcal{B} (10^{-6})
ωK^{*0}	$32.9^{+13.0}_{-12.0}$	2.91	0.94	3.0	$1.8 \pm 0.7^{+0.3}_{-0.2}$
$\omega K^+\pi^-$	$146.5^{+20.4}_{-19.3}$	4.66	0.94	9.5	$5.1 \pm 0.7 \pm 0.7$

sum of two Gaussians is used to describe M_{bc} . To take into account small differences between the MC and data, the M_{bc} and ΔE shapes for the signal and $\omega K^+\pi^-$ PDFs are corrected according to calibration factors determined from a large $B^0 \rightarrow D^-\rho^+$, $D^- \rightarrow K^+\pi^-\pi^-$ control sample. The $M_{K\pi}$ PDF for $\omega K^+\pi^-$ decays is represented by a threshold function with parameters determined from MC events where the $K\pi$ final state is distributed uniformly over phase space.

For the $q\bar{q}$ background, we use a threshold ARGUS [15] function to describe M_{bc} , and linear functions to describe ΔE and the combinatorial shapes of $M_{\pi\pi\pi}$ and $M_{K\pi}$. The M_{bc} and ΔE shapes of the $b \rightarrow c$ background are described by an ARGUS function and a second-order Chebyshev polynomial, respectively. The remaining PDF shapes are modeled with non-parametric PDFs using Kernel Estimation [16].

The following parameters vary in our final fit to the data: the signal, $\omega K^+\pi^-$, $b \rightarrow c$ and $q\bar{q}$ yields, and the $q\bar{q}$ PDF parameters describing the ΔE , M_{bc} and combinatorial shapes of $M_{\pi\pi\pi}$ and $M_{K\pi}$. The fraction of $b \rightarrow s, u, d$ events ($f_{b \rightarrow s, u, d}$) is small (1.6%) and fixed to the MC value. The f_{SCF} for signal and $\omega K^+\pi^-$ decays are also fixed to their MC values.

The fit results are listed in Table I and the projections are shown in Fig. 1. With the fitted yields Y , we calculate the branching fraction \mathcal{B} as $Y/(\varepsilon_{\text{MC}} \cdot \varepsilon_{\text{PID}} \cdot N_{B\bar{B}})$, where ε_{MC} is the event selection efficiency including daughter branching fractions obtained from MC simulation, $N_{B\bar{B}}$ is the number of $B\bar{B}$ pairs produced, and ε_{PID} is an efficiency correction for the charged track selection that takes into account small differences between MC and data. Our signal MC is generated with $f_L = 0.5$; the change in acceptance for other values of f_L is taken as a systematic error. For $\omega K^+\pi^-$, ε_{MC} and \mathcal{B} are for $M_{K\pi} \in (0.755, 1.250)$ GeV/ c^2 .

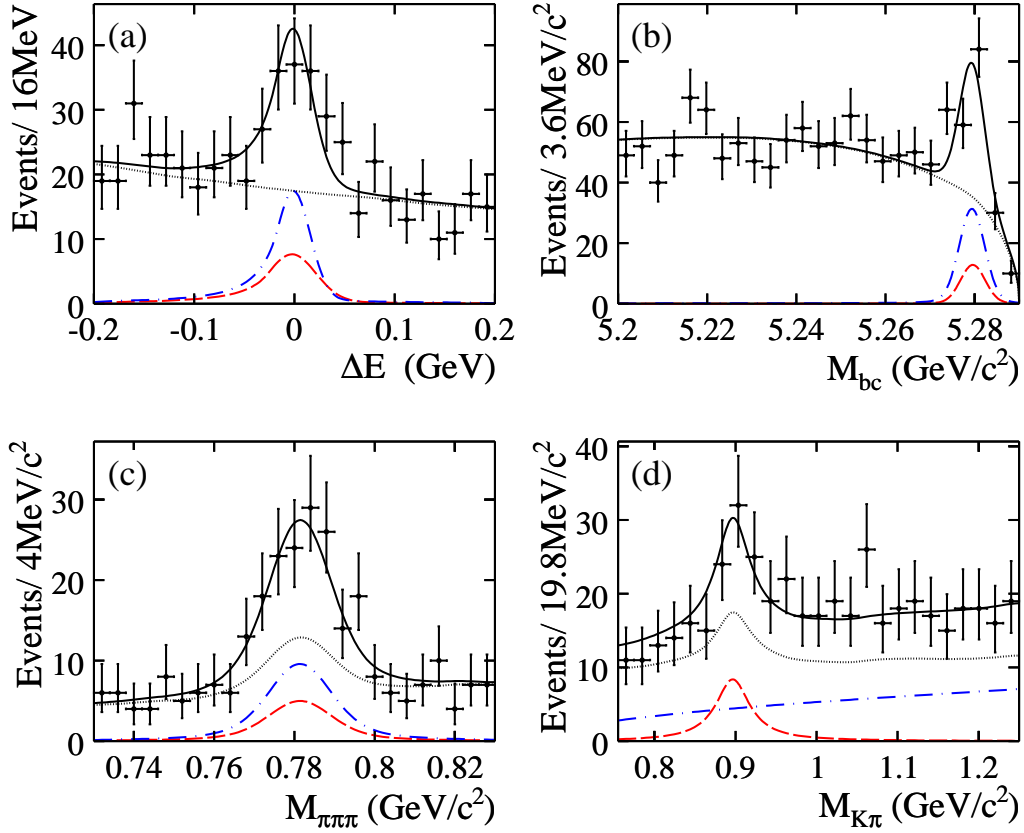


FIG. 1: Projections of the fit results onto (a) ΔE , (b) M_{bc} , (c) $M_{\pi\pi\pi}$ and (d) $M_{K\pi}$ for candidates satisfying (except for the variable plotted) the criteria $\Delta E \in (-0.10, 0.06)$ GeV, $M_{bc} \in (5.27, 5.29)$ GeV/ c^2 and $M_{K\pi} \in (0.755, 1.050)$ GeV/ c^2 . The curves are for ωK^{*0} (dashed), $\omega K^+\pi^-$ (dot-dashed), the sum of the backgrounds (dotted), and the total (solid).

The significance is defined as $\sqrt{-2\ln(\mathcal{L}_0/\mathcal{L}_{\max})}$, where \mathcal{L}_{\max} (\mathcal{L}_0) is the value of the likelihood function when the yield is allowed to vary (set to 0). The systematic uncertainty is included by convolving the likelihood function with a Gaussian whose width is equal to the systematic error. For signal and $\omega K^+\pi^-$ decays, we account for small correlations between the fitted variables by fitting ensembles of simulated experiments containing all signal and background components. The correlations give rise to biases of +2.9 and +8.1 events for signal and $\omega K^+\pi^-$, respectively. We correct the fitted yields for these biases.

We study the effects of interference between $B^0 \rightarrow \omega K^{*0}$ and $B^0 \rightarrow \omega K^+\pi^-$ decays as follows. We modify the Breit-Wigner PDF describing the K^{*0} resonance of the signal to include an interfering amplitude and phase; for lack of more information, we take this

amplitude to be constant in $M_{K\pi}$. We uniformly vary the amplitude and phase from zero to a maximum and, for each case, generate and fit a large ensemble of toy MC experiments. The r.m.s. spread of deviations about the true value is taken as the systematic error ($^{+0.9\%}_{-1.1\%}$ for ωK^{*0}).

The remaining sources of systematic error for the branching fraction include: track reconstruction efficiency (1.2% per track); π^0 efficiency (4%); PID (1.3%); $N_{B\bar{B}}$ (1.4%); MC statistics (0.6%); PDF shapes ($^{+5.9\%}_{-6.8\%}$); $f_{b\rightarrow s,u,d}$ (2.6%); f_{SCF} ($^{+5.7\%}_{-5.2\%}$); the ΔE fit range ($^{+5.0\%}_{-0.0\%}$); fitting bias (7.8%); the effect of higher K^{*0} resonances ($^{+1.8\%}_{-0.0\%}$); f_L ($^{+0.8\%}_{-1.3\%}$); and $\mathcal{R}_{q\bar{q}}$ (2.8%). The errors on the PDF shapes are obtained by varying all fixed parameters by $\pm 1\sigma$. To obtain the error due to f_{SCF} and $f_{b\rightarrow s,u,d}$, we vary these fractions by $\pm 50\%$. The uncertainty in the yield bias correction is taken to be the sum in quadrature of the statistical uncertainty on the correction and half the correction value. We consider the effects of higher K^{*0} resonances by including a PDF for $B^0 \rightarrow \omega K_0^*(1430)^0$ and repeating the 4D fit with the $\omega K_0^*(1430)^0$ yield fixed to the value obtained by extrapolating from a higher $M_{K\pi}$ region. The error due to the uncertainty in f_L is obtained by varying f_L by its errors measured below. To obtain the uncertainty due to the $\mathcal{R}_{q\bar{q}}$ requirement, we vary the $\mathcal{R}_{q\bar{q}}$ thresholds, and we also calculate the data/MC efficiency ratio for the $B^0 \rightarrow D^-\rho^+$, $D^- \rightarrow K^+\pi^-\pi^-$ control sample. Combining all errors in quadrature gives a total systematic error of ($^{+14.7\%}_{-14.0\%}$). The systematic errors considered for $\omega K^+\pi^-$ are similar; the total is ($^{+13.9\%}_{-13.8\%}$).

To verify the large $\omega K^+\pi^-$ contribution (see Table I), we bin the data in $M_{K\pi}$ from 0.65 – 1.25 GeV/ c^2 and, for each bin, perform a two-dimensional (2D) fit to ΔE and M_{bc} .

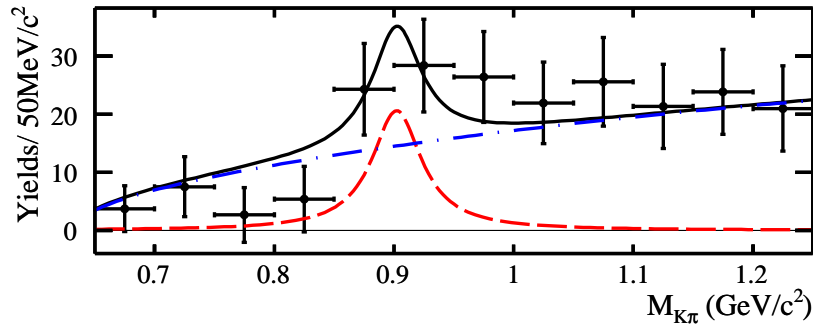


FIG. 2: Signal + $\omega K^+\pi^-$ yields obtained from 2D fits to ΔE and M_{bc} in bins of $M_{K\pi}$. The curves are for ωK^{*0} (dashed), $\omega K^+\pi^-$ (dot-dashed), and the total (solid).

The likelihood function consists of three components: signal + $\omega K^+\pi^-$, $q\bar{q} + b \rightarrow c$, and $b \rightarrow s, u, d$. We plot the resulting yields of signal + $\omega K^+\pi^-$ as a function of $M_{K\pi}$ (Fig. 2) and fit this distribution to extract the signal and $\omega K^+\pi^-$ components. For $M_{K\pi} \in (0.755, 1.250)$ GeV/ c^2 we obtain yields of 29.3 ± 12.1 and 161.5 ± 16.3 for signal and $\omega K^+\pi^-$, respectively; these values are in good agreement with the results of the 4D fit after accounting for the fit bias.

The differential decay width, after integrating over the angle between the decay planes of the ω and K^{*0} mesons, is proportional to $(1 - f_L) \sin^2 \theta_\omega \sin^2 \theta_{K^{*0}} + 4f_L \cos^2 \theta_\omega \cos^2 \theta_{K^{*0}}$. Here, the fraction of longitudinal polarization $f_L \equiv |A_0|^2 / \sum_\lambda |A_\lambda|^2$, where A_λ are the helicity amplitudes for the longitudinal ($\lambda = 0$) and transverse ($\lambda = \pm 1$) states [17]. To determine f_L , we bin the data in $|\cos \theta_\omega|$ and $\cos \theta_{K^{*0}}$ and, for each bin, perform a 4D fit to ΔE , M_{bc} , $M_{K\pi}$, and $M_{\pi\pi\pi}$. The resulting signal yields as a function of the helicity cosines are shown in Fig. 3. We perform a simultaneous χ^2 fit to these distributions, where the only floating parameter is f_L . The PDFs for the A_0 and $A_{\pm 1}$ helicity states are determined from MC simulation to take into account the detection efficiency. The statistical error is obtained from a toy MC study since the errors in the distributions of Fig. 3 are correlated. Using a large toy MC sample we measure a 2% bias in the fitting procedure, which we use to correct the central value.

There are six main sources of systematic error in f_L : uncertainty in the PDF shapes (+0.16, -0.06); the fractions $f_{b \rightarrow s, u, d}$ (+0.02, -0.01) and f_{SCF} (+0.01, -0.01); fitting bias (+0.02, -0.00); interference (+0.02, -0.01); and the $\mathcal{R}_{q\bar{q}}$ requirement (+0.08, -0.05). Adding the various systematic contributions in quadrature, we obtain a longitudinal polarization fraction

$$f_L(B^0 \rightarrow \omega K^{*0}) = 0.56 \pm 0.29(\text{stat})_{-0.08}^{+0.18}(\text{syst}). \quad (2)$$

In summary, using 657×10^6 $B\bar{B}$ pairs we have found evidence for the $B^0 \rightarrow \omega K^{*0}$ decay with a significance of 3.0σ . We measure the branching fraction to be $\mathcal{B}(B^0 \rightarrow \omega K^{*0}) = [1.8 \pm 0.7(\text{stat})_{-0.2}^{+0.3}(\text{syst})] \times 10^{-6}$. Our result is in agreement with theoretical estimates [5]. We also perform a helicity analysis of the ω and K^{*0} vector mesons and measure a longitudinal polarization fraction $f_L(B^0 \rightarrow \omega K^{*0}) = 0.56 \pm 0.29(\text{stat})_{-0.08}^{+0.18}(\text{syst})$. This central value is lower than that predicted by most theoretical models but is similar to that measured for other $b \rightarrow sq\bar{q}$ decays [1]. In addition, we measure a large non-resonant branching fraction $\mathcal{B}(B^0 \rightarrow \omega K^+\pi^-; M_{K\pi} \in (0.755, 1.250) \text{ GeV}/c^2) = [5.1 \pm 0.7(\text{stat}) \pm 0.7(\text{syst})] \times 10^{-6}$ with a

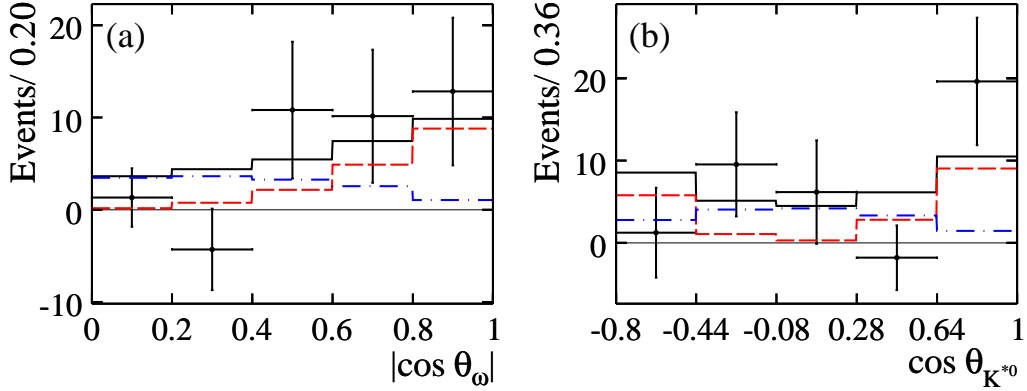


FIG. 3: Signal yields obtained from 4D fits to ΔE , M_{bc} , $M_{K\pi}$, and $M_{\pi\pi\pi}$, in bins of (a) $|\cos \theta_\omega|$ and (b) $\cos \theta_{K^*0}$. The solid histograms show the results of the simultaneous χ^2 fit. The dashed (dot-dashed) histograms are the A_0 ($A_{\pm 1}$) component.

significance of 9.5σ . Assuming a uniform phase space distribution, this implies a branching fraction of $[79^{+11}_{-10}(\text{stat}) \pm 11(\text{syst})] \times 10^{-6}$ over the whole region.

We thank the KEKB group for excellent operation of the accelerator, the KEK cryogenics group for efficient solenoid operations, and the KEK computer group and the NII for valuable computing and SINET3 network support. We acknowledge support from MEXT and JSPS (Japan); ARC and DEST (Australia); NSFC (China); DST (India); MOEHRD, KOSEF and KRF (Korea); KBN (Poland); MES and RFAAE (Russia); ARRS (Slovenia); SNSF (Switzerland); NSC and MOE (Taiwan); and DOE (USA).

* now at Okayama University, Okayama

- [1] Belle Collaboration, K.F. Chen *et al.*, Phys. Rev. Lett. **94**, 221804 (2005). Belle Collaboration, J. Zhang *et al.*, Phys. Rev. Lett. **95**, 141801 (2005); BaBar Collaboration, B. Aubert *et al.*, Phys. Rev. Lett. **97**, 201801 (2006); BaBar Collaboration, B. Aubert *et al.*, Phys. Rev. Lett. **98**, 051801 (2007); BaBar Collaboration, B. Aubert *et al.*, Phys. Rev. Lett. **99**, 201802 (2007).
- [2] BaBar Collaboration, B. Aubert *et al.*, Phys. Rev. Lett. **99**, 021603 (2007). Belle Collaboration, S.-W. Lin *et al.*, Nature **452**, 332 (2008).
- [3] A. Kagan, Phys. Lett. B **601**, 151 (2004); C. Bauer *et al.*, Phys. Rev. D **70**, 054015 (2004); P. Colangelo *et al.*, Phys. Lett. B **597**, 291 (2004); M. Ladisa *et al.*, Phys. Rev. D **70**, 114025 (2004).

- (2004); H.-n. Li and S. Mishima, Phys. Rev. D **71**, 054025 (2005); M. Beneke *et al.*, Phys. Rev. Lett. **96**, 141801 (2006); H. Y. Cheng and K.C. Yang, arXiv:0805.0329.
- [4] D. Atwood and A. Soni, Phys. Rev. D **59**, 013007 (1998); D. Atwood and A. Soni, Phys. Rev. D **65**, 073018 (2002); H.-W. Huang *et al.*, Phys. Rev. D **73**, 014011 (2006).
- [5] A. Ali, G. Kramer, and C.-D. Lü, Phys. Rev. D **58**, 094009 (1998); Y.H. Chen *et al.*, Phys. Rev. D **60**, 094014 (1999); H. Y. Cheng and K.C. Yang, Phys. Lett. B **511**, 40 (2001); W. Zou and Z. Xiao, Phys. Rev. D **72**, 094026 (2005); M. Beneke, J. Rohrer and D. Yang, Nucl. Phys. B **774**, 64 (2007).
- [6] BaBar Collaboration, B. Aubert *et al.*, Phys. Rev. D **74**, 051102 (2006).
- [7] Belle Collaboration, A. Abashian *et al.*, Nucl. Instrum. Methods Phys. Res., Sect. A **479**, 117 (2002).
- [8] S. Kurokawa and E. Kikutani, Nucl. Instrum. Methods Phys. Res., Sect. A **499**, 1 (2003), and other papers in this volume.
- [9] Charge-conjugate decays are included unless explicitly stated otherwise.
- [10] The Fox-Wolfram moments were introduced in G. C. Fox and S. Wolfram, Phys. Rev. Lett. **41**, 1581 (1978). The modified moments used in this Letter are described in Belle Collaboration, S. H. Lee *et al.*, Phys. Rev. Lett. **91**, 261801 (2003).
- [11] H. Kakuno *et al.*, Nucl. Instrum. Methods Phys. Res., Sect. A **533**, 516 (2004).
- [12] Evtgen generator, D. J. Lange, Nucl. Instrum. Methods Phys. Res., Sect. A **462**, 152 (2001). The detector response is simulated with GEANT, R. Brun *et al.*, GEANT 3.21, CERN Report DD/EE/84-1, 1984.
- [13] Particle Data Group, W.-M. Yao *et al.*, J. Phys. G **33**, 1 (2006).
- [14] T. Skwarnicki, Ph.D. Thesis, Institute for Nuclear Physics, Krakow 1986; DESY Internal Report, DESY F31-86-02 (1986).
- [15] ARGUS Collaboration, H. Albrecht *et al.*, Phys. Lett. B **241**, 278 (1990).
- [16] Kernel Estimation in High-Energy Physics, K. Cranmer, Comput. Phys. Commun. **136** (2001) 198207, hep-ex/0011057.
- [17] K. Abe, M. Sapaty, and H. Yamamoto, hep-ex/0103002.